THE JOURNAL OF PHYSICAL CHEMISTRY A

Article

pubs.acs.org/JPCA

Electronic Absorption Spectrum of Triacetylene Cation for Astronomical Considerations

S. Chakrabarty, C. A. Rice, F. J. Mazzotti, R. Dietsche, and J. P. Maier*

Department of Chemistry, University of Basel, Klingelbergstr. 80, CH-4056 Basel, Switzerland

ABSTRACT: The $A^2\Pi_g \leftarrow X^2\Pi_u$ electronic transition (4800−6000 Å) of triacetylene cation was measured in an ion trap, where the vibrational and rotational degrees of freedom were equilibrated to 25 K. The rotational profile of the origin band is predicted by a collisional-radiative rate model under conditions expected in diffuse interstellar clouds. Variation in the density of the surrounding gas, rotational temperature, and velocity dispersion are taken into account.

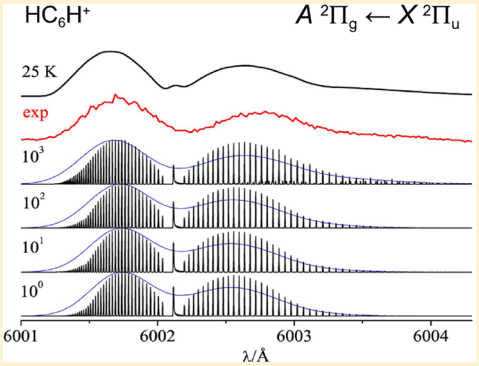

1. INTRODUCTION

Diffuse absorption features were recognized in the spectra of O- and B-type stars nearly a century ago.[1] Since then, over 600 diffuse interstellar bands (DIBs) have been catalogued in the visible region of the electromagnetic spectrum; they vary in width (fwhm) from tens of Å to just a fraction of one.[2] It is generally considered that the DIB carriers are gaseous molecules or ions, which may be carbonaceous in nature given the large abundance of C in the interstellar medium (ISM).[3] A challenging aspect of determining whether a DIB is due to a particular molecular species is that more than one absorption feature of an electronic transition must coincide with DIBs in the 4000−9000 Å region.[4]

With the knowledge of the spectroscopic constants obtained from a laboratory spectrum, a synthetic band profile can be compared to the astronomical trace, taking into account the physical conditions of the ISM. This includes rotational and kinetic temperatures, gas densities, and velocity broadening of the molecular cloud in a line of sight. The rotational level populations can be calculated by considering (1) radiative decay of allowed transitions, (2) collisional rates with hydrogen, and (3) 2.7 K cosmic background radiation.

The rotational profiles of the origin bands of electronic transitions of several carbon-bearing molecules, e.g., $C_{2n}H$ (n = 3−6), $HC_{2n}H^+$ (n = 2−4), and $NC_{2n-2}N^+$ (n = 3, 4), have been simulated at various rotational temperatures for comparison with astrophysical data, assuming a Boltzmann distribution.[5] The band maxima, as well as the peak widths, change with temperature. For example, a Boltzmann distribution at 3 K and a velocity broadening of 15 km s^{-1} would result in a single feature for the origin band of C_6H, while a temperature slightly higher than 10 K would result in a double band. In addition, at ≥10 K, a weak blueshifted absorption appears, due to the Ω = 1/2 spin−orbit component, and at 150 K, two comparable intensity peaks are seen.[5] In a recent article dealing with the $A^2\Pi_u \leftarrow X^2\Pi_g$ electronic spectrum of HC_4H^+, it was pointed out that processes such as magnetic dipole transitions will distort the Boltzmann population and hence the profile.[6]

In this contribution, the $A^2\Pi_g \leftarrow X^2\Pi_u$ electronic spectrum of triacetylene cation has been measured in an ion trap at 25 K by a two-photon excitation−dissociation technique. The rotational profile of the origin band under typical interstellar conditions is predicted. The population in the ISM is non-Boltzmann because the $^2\Pi_{1/2}$ spin−orbit component will be depopulated by magnetic dipole transitions ($^2\Pi_{1/2} \rightarrow {}^2\Pi_{3/2}$). The theory of this has been worked out.[7] The population and rotational profile are modeled considering the magnetic dipole transitions, 2.7 K blackbody radiation, and collisional rates.

2. METHODS

2.1. Experimental Section. The apparatus employed has been explained.[8] An electrostatic quadrupole deflector has been incorporated after the first mass filter directly before the 22-pole ion trap, allowing for easier laser access. Mass-selected ions are deflected into the trap and, after thermalization followed by laser irradiation, extracted and analyzed by a second quadrupole mass selector.

HC_6H^+ was generated by 30 eV electron bombardment of gaseous diacetylene. Ions were stored for ∼60 ms, and a few thousand ions were trapped per duty cycle. Visible radiation from a tunable laser (fwhm 1.2 Å at 6000 Å) was used to resonantly excite the $A^2\Pi_g \leftarrow X^2\Pi_u$ electronic transition,

Special Issue: Oka Festschrift: Celebrating 45 Years of Astrochemistry

Received: December 13, 2012
Revised: March 4, 2013

   dx.doi.org/10.1021/jp312294f | J. Phys. Chem. A XXXX, XXX, XXX−XXX

whereas subsequent irradiation with a UV laser (fwhm 0.6 Å at 2660 Å) led to detectable fragmentation yields.

2.2. Model. A radiative-collisional model was used to calculate the population of the rotational and spin−orbit levels in the $X^2\Pi_u$ ground state of HC_6H^+. Expressions for the upward collisional rates were used from a modified exponential gap model:[9]

$$k_{up}(i, j, T) = \alpha(T)\left(\left(1 + \frac{aE_i}{kT\delta}\right)\left(1 + \frac{aE_i}{kT}\right)^{-1}\right)^2 \exp\left(-\frac{\beta E_{ij}}{kT}\right)$$

where $\alpha(T) = pAT^{-B}$; p is the thermodynamic pressure, A = 23.2 and B = 1.36, a = 2, k = Boltzmann constant, T = kinetic temperature, δ = 1.59, and β = 5 extrapolated from the values HCl (1.43),[10] CO (1.5),[11] HCN (1.23),[12] and HC_3N (3.89)[11] with helium impingement. The downward collisional rates are[13]

$$k_{down}(j, i, T) = k_{up}(i, j, T)\left(\frac{2i + 1}{2j + 1}\right)\left(\frac{m_i}{m_j}\right)\exp\left(\frac{E_{ij}}{kT}\right)$$

where m_i/m_j are the nuclear spin statistical weights for levels i and j. This is 3:1 for antisymmetric (a) and symmetric (s) levels, respectively.

The 2.7 K blackbody background radiation gives rise to absorption and stimulated emission of a photon for the allowed transitions (Figure 1), given by

$$k_{stim,ji} = \frac{A_{ji}}{e^{E_{ij}/kT} - 1} \qquad k_{abs,ij} = \left(\frac{2j + 1}{2i + 1}\right)\frac{m_j}{m_i}\left(\frac{A_{ji}}{e^{E_{ij}/kT} - 1}\right)$$

where A_{ji} is the Einstein coefficient of spontaneous emission.

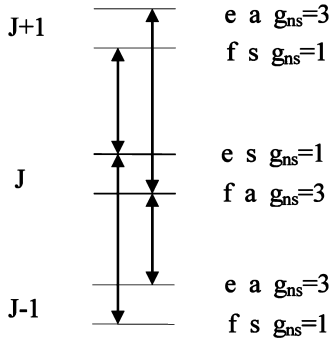

Figure 1. Considered processes connecting rotational J levels in the electronic $^2\Pi_{u,3/2}$ ground state by magnetic dipole and collision-induced transitions, as well as the stimulated emission and absorption of 2.7 K cosmic background radiation.

Collisional rates were considered only between s−s and a−a levels, neglecting the a−s and s−a transitions, with the assumption that these are much smaller. In the Ω = 3/2 manifold, J = 3/2 (lowest level) has a 3:1 a/s ratio through all Ω and J. Figure 1 shows an energy level diagram of the possible upward and downward magnetic dipole and collisional transitions within the Ω = 3/2 manifold. J−3/2 is even, and this imposes the symmetry of the e/f levels as well as their respective nuclear spin statistics (g_{ns}). The upper spin−orbit manifold is completely depopulated for the range of densities considered when the collision-induced ΔΩ ± 1 transitions are neglected.

Because triacetylene cation has no permanent dipole moment, only magnetic dipole transitions couple adjacent j levels (Figure 1). The radiative rates were calculated with the PGOPHER program[14] for a magnetic dipole transition of the $X^2\Pi_u$ ground state of HC_6H^+. The expression for the transition moment operator was from ref 7.

3. RESULTS AND DISCUSSION

3.1. Electronic Spectrum of Triacetylene Cation. The electronic spectrum of HC_6H^+ has been measured at 25 K. Both vibrational and rotational degrees of freedom were equilibrated to such a low temperature by confining mass-selected ions in a 22-pole radio frequency trap, while they underwent collisions with cryogenically cooled helium. Absorptions were induced by a two-color, two-photon excitation−dissociation scheme. In Figure 2, the relevant levels

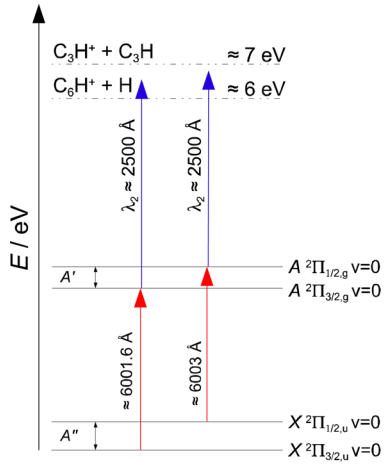

Figure 2. Energy level diagram of the $X^2\Pi_u$ ground and $A^2\Pi_g$ excited electronic states involved in the optical transition of HC_6H^+ along with different dissociation pathways. The longer wavelengths are the maxima of the R_{11} and R_{22} branches.

involved are given. There are three important considerations for such measurements in an ion trap: (1) The rotational and vibrational degrees of freedom are equilibrated by collisions, which is not necessarily the case in supersonic jet expansions[15] where T_{rot} is low but the vibrational degrees of freedom may not be. (2) Because of the mass-selection, species (e.g., C_2, C_3) produced concomitantly with the ions are absent, and thus, their absorptions do not overlap in the spectrum. (3) The ion trap measurement is not a linear absorption technique; the intensity depends on the cross-section for the $A^2\Pi_g \leftarrow X^2\Pi_u$ excitation and the rate of photofragmentation.

The first mass filter ensured that the only species transported to the trap was HC_6H^+. Figure 3A shows the resonant two-color, two-photon fragmentation (R2C2PF) recording of the $A^2\Pi_g \leftarrow X^2\Pi_u$ electronic spectrum of HC_6H^+ obtained by counting the laser-induced dissociation product as a function of wavelength. The loss of H atom probably proceeds through a direct unimolecular bond cleavage mechanism, whereas $C_3H_2^+$ formation can be envisaged through a rearrangement/isomerization of the parent ion near the fragmentation threshold. Trace B in Figure 3 is the laser excitation spectrum of this electronic transition of HC_6H^+ measured before.[15] The quantum yield of fluorescence of HC_6H^+ does not change appreciably across the measured energy range (4800−6000 Å), making this a reference for the photofragmentation spectrum. The comparison reveals anomalies in the intensities of the 3_0^1/

dx.doi.org/10.1021/jp312294f | J. Phys. Chem. A XXXX, XXX, XXX−XXX

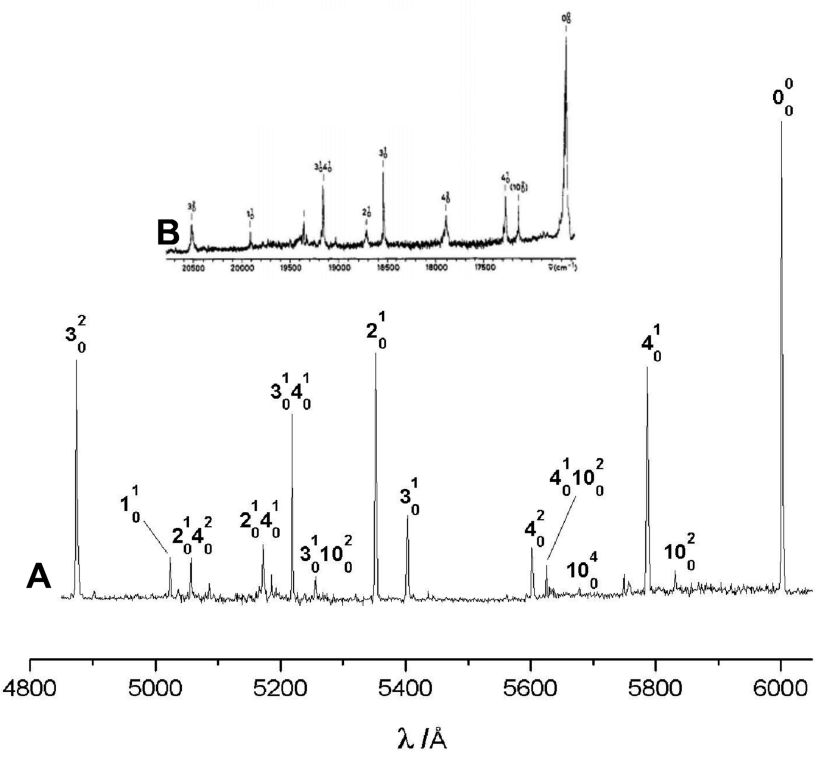

Figure 3. Trace **A**: The $A^2\Pi_g \leftarrow X^2\Pi_u$ electronic absorption spectrum of HC_6H^+ measured at 25 K by the resonant two-color, two-photon dissociation method, counting the C_3^+, C_3H^+, and $C_3H_2^+$ fragments. Trace **B** is the laser induced fluorescence spectrum of this transition at ~100 K reproduced from ref 15. The reduced line width of the absorptions in trace **A** is because of the lower vibrational and rotational temperatures achieved in the ion trap.

2_0^1 bands in the latter spectrum. In the R2C2PF process, the fragmentation rate is not constant but a function of the internal energy of the parent ion. The spectrum is dominated by the origin band and shows progressions in the ν_3 and ν_4 symmetric stretching modes in the $A^2\Pi_g$ excited state. The transitions originate from the v = 0 level of the $X^2\Pi_u$ ground electronic state at a temperature of 25 K. Hot bands that would arise because of residual population of the low frequency modes ($\nu_{13} \approx 100$ cm^{-1}) were not detected, indicating that the ions were vibrationally relaxed with a population of ~0.3% of v = 0 at 25 K.

The profile of the origin band in the $A^2\Pi_g \leftarrow X^2\Pi_u$ transition was measured and compared to simulations using the known spectroscopic constants,[16] to confirm that the rotational temperature of the ions was 25 K.[14] The constants used were B'' = 0.044 594 cm^{-1} and B' = 0.043 792 cm^{-1}. The $X^2\Pi_u$ and $A^2\Pi_g$ electronic states have two spin−orbit components Ω = 1/2 and 3/2 (inverted); A'' = −31.4 cm^{-1} and A' = −28.41 cm^{-1}. At 25 K, the v = 0 level of $X^2\Pi_{1/2}$ has only ~15% population compared to v = 0 of $X^2\Pi_{3/2}$. This is apparent in the spectrum in Figure 4 where the shoulder in the unresolved *P* branch is the much weaker transition originating from the Ω = 1/2 spin−orbit component.

3.2. Origin Band Profile for Astronomy. The results from the model, including radiative and collisional rates, show that the rotational level population has a non-Boltzmann distribution, when a hydrogen density of 1 cm^{-3} and a kinetic temperature of 60 K is considered. As the rotational energy reaches the Ω = 1/2 manifold (31.4 cm^{-1}), a slight nonlinearity occurs where the *J* levels of the two spin−orbit components cross. In the case where there is no collisional electronic spin

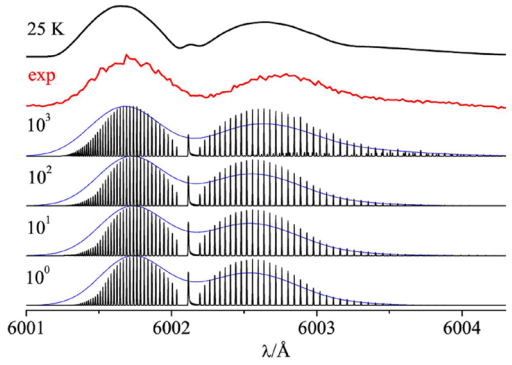

Figure 4. Origin band of the $A^2\Pi_g \leftarrow X^2\Pi_u$ electronic transition of HC_6H^+ recorded with a 0.05 Å laser bandwidth by a resonant two-color, two-photon fragmentation technique is shown in red. The predicted rotational profiles of this band as a function of collision partner density in cm^{-3}, showing individual *J* lines with a 0.007 Å fwhm at 6000 Å in black, and a velocity dispersion of 18 km s^{-1} are overlaid in blue. The top trace is the simulated profile, using a Gaussian of 0.1 Å for each rotational line and a Boltzmann temperature of 25 K.

conversion, the slope is monotonic with increasing rotational level energy and Boltzmann in nature.

When the radiative rates for different rotational states are considered, R_{22} and R_{11}, and the three $\Delta\Omega$ = +1 branches have to be taken into account. However, the Ω = 1/2 ← 3/2 Q_{21}, R_{21}, and P_{21} branches have a ν^3 dependence as given by the Einstein A_{ji} coefficient. The Ω = 1/2 ← 3/2 radiative rates are greater than collisional ones (for β_{MEG} = 5) for the density range (1−10^3 cm^{-3}) considered,[17] indicating that the Ω = 1/2

dx.doi.org/10.1021/jp312294f | J. Phys. Chem. A XXXX, XXX, XXX−XXX

population will be governed by radiative processes. Furthermore, as upward collisional rates follow an exponential decay with increasing transition energy, the rates associated with R_{11} and R_{22} become dominant. This causes a drop in temperature with increasing J.

The spectral profile of the $A^2\Pi_g \leftarrow X^2\Pi_u$ electronic transition of HC_6H^+ has been simulated with a line width equivalent to 18 km s^{-1} cloud velocity dispersion using the rotational distribution calculated by the code described in section 2.2. The rotational temperatures of the two spin−orbit components are reported in Table 1 as a ratio between $\Omega = 3/2$ and 1/2. For low rotational temperatures, i.e., negligible collisions, the profile is nearly a single peak. This is the case when the cation is equilibrated to the 2.7 K blackbody radiation. At higher temperatures, the P_{11} and R_{11} branches (Figure 4) start to split into two distinct features. The $\Omega = 1/2$ component appears in the spectrum at higher densities because the collisional rates are faster than the radiative ones. The predicted band maxima of the Gaussian fits are listed in Table 1.

Table 1. Predicted Spectral Characteristics of the Origin Band in the $A^2\Pi_g \leftarrow X^2\Pi_u$ Transition of HC_6H^+ Using the Model Described in Text[a]

N (cm^{-3})	T_{rot} (K) Ω = 1.5:0.5	band max (Å) (±0.05 Å)	fwhm (Å)
10^{-5}	2.7:2.7	6002.08	0.64
10^{-3}	3.5:4.2	6001.90	0.42
		6002.30	0.49
10^{0}	14.1:7.0	6001.73	0.51
		6002.54	0.80
10^{2}	15.6:8.9	6001.71	0.51
		6002.56	0.84
10^{3}	21.1:15.3	6001.68	0.54
		6002.61	0.79
		6003.22	1.15
10^{5}	54.3:52.5	6001.49	0.57
		6002.60	0.63
		6003.39	2.13

[a]These were obtained by fitting R_{11}, P_{11}, and $\Omega = 1/2$ spin-orbit component by Gaussian lineshapes of variable widths and maxima (up to three for higher rotational temperatures). The spectra were calculated with a 60 K kinetic temperature, a 18 km s^{-1} velocity dispersion, and $\beta = 5$.

In summary, modeling of the ground state rotational population shows the following:

(1) The temperature is smaller than the kinetic one of the surrounding gas up to a threshold of the dimensionless parameter $\rho \approx 107$, where $\rho = (N \times \alpha(60K))/2.5A_{j,j-1}$.
(2) Exclusion of spin conversion by collisions results in depopulation of the $\Omega = 1/2$ component. The spin−orbit temperature is then equilibrated with the 2.7 K blackbody radiation in the range of densities considered.
(3) The rotational temperatures are only estimates because of nonlinearity of the Boltzmann plots.

4. CONCLUSIONS

The $A^2\Pi_g \leftarrow X^2\Pi_u$ electronic spectrum of HC_6H^+ has been remeasured using a resonant two-color, two-photon photofragmentation technique in an ion trap at 25 K. Blackbody radiation, collisional rates, and magnetic dipole transitions have been taken into account to predict the rotational profile of the origin band under expected conditions in the diffuse interstellar clouds. These aspects should be considered when comparing laboratory absorption spectra with astronomical data.

AUTHOR INFORMATION

Corresponding Author

*E-mail: j.p.maier@unibas.ch. Tel: +41 61 267 38 26. Fax: +41 61 267 38 55.

Notes

The authors declare no competing financial interest.

ACKNOWLEDGMENTS

This work was supported by the Swiss National Science Foundation (Project No. 200020-140316/1) and the European Research Council (ERC-AdG-ElecSpecIons:246998).

REFERENCES

(1) Herbig, G. H. The Diffuse Interstellar Bands. *Annu. Rev. Astrophys.* **1995**, *33*, 19−73.
(2) Hobbs, L. M.; York, D. G.; Snow, T. P.; Oka, T.; Thorburn, J. A.; Bishof, M.; Friedman, S. D.; McCall, B. J.; Rachford, B.; Sonnentrucker, P.; et al. A Catalog of Diffuse Interstellar Bands in the Spectrum of HD 204827. *Astrophys. J.* **2008**, *680*, 1256−1270.
(3) Oka, T.; McCall, B. J. Disclosing Identities in Diffuse Interstellar Bands. *Science* **2011**, *331*, 293−294.
(4) Jochnowitz, E. B.; Maier, J. P. Electronic Spectroscopy of Carbon Chains. *Annu. Rev. Phys. Chem.* **2008**, *59*, 519−544.
(5) Motylewski, T.; Linnartz, H.; Vaizert, O.; Maier, J. P.; Galazutdinov, G. A.; Musaev, F. A.; Krełowski, J.; Walker, G. A. H.; Bohlender, D. A. Gas-Phase Electronic Spectra of Carbon-Chain Radicals Compared with Diffuse Interstellar Band Observations. *Astrophys. J.* **2000**, *531*, 312−320.
(6) Maier, J. P.; Chakrabarty, S.; Mazzotti, F. J.; Rice, C. A.; Dietsche, R.; Walker, G. A. H.; Bohlender, D. A. Assignment of 5069 Å Diffuse Interstellar Band to HC_4H^+: Disagreement with Laboratory Absorption Band. *Astrophys. J. Lett.* **2011**, *729*, L20.
(7) Morse, M. D.; Maier, J. P. Detection of Nonpolar Ions in $^2\Pi_{3/2}$ States by Radioastronomy via Magnetic Dipole Transitions. *Astrophys. J.* **2011**, *732*, 103.
(8) Rudnev, V.; Rice, C. A.; Maier, J. P. $B^2\Sigma_u^+ - X^2\Pi_g$ Electronic Spectrum of $NCCN^+$ in the Gas Phase. *J. Chem. Phys.* **2008**, *129*, 134315.
(9) Belikov, A. E.; Smith, M. A.. State-to-State Rate Coefficients for Rotational Relaxation of CO in Ar. *J. Chem. Phys.* **1999**, *110*, 8513−8524.
(10) Neufeld, D. A.; Green, S. Excitation of Interstellar Hydrogen-Chloride. *Astrophys. J.* **1994**, *432*, 158−166.
(11) Green, S.; Chapman, S. Collisional Excitation of Interstellar Molecules: Linear-Molecules CO, CS, OCS, and HC_3N. *Astrophys. J. Suppl. Ser.* **1978**, *37*, 169−194.
(12) Green, S.; Thaddeus, P. Rotational Excitation of HCN by Collisions. *Astrophys. J.* **1974**, *191*, 653−657.
(13) Lique, F.; Spielfiedel, A.; Dubernet, M. L.; Feautrier, N. Rotational Excitation of Sulfur Monoxide by Collisions with Helium at Low Temperature. *J. Chem. Phys.* **2005**, *123*, 134316.
(14) Western, C. M. *PGOPHER*, a Program for Simulating Rotational Structure; University of Bristol: Bristol, U.K., 2007; see http://pgopher.chm.bris.ac.uk.
(15) Klapstein, D.; Kuhn, R.; Maier, J. P.; Ochsner, M.; Zambach, W. Emission and Laser Excitation Spectra of the $A\ ^2\Pi_g \leftrightarrow X\ ^2\Pi_u$ Transition of Rotationally Cooled Triacetylene Cation. *J. Phys. Chem.* **1984**, *88*, 5176−5180.
(16) Cias, P.; Vaizert, O.; Denisov, A.; Mes, J.; Linnartz, H.; Maier, J. P. Electronic Gas-Phase Spectrum of the Pentaacetylene Cation. *J. Phys. Chem. A* **2002**, *106*, 9890−9892.
(17) Snow, T. P.; McCall, B. J. Diffuse Atomic and Molecular Clouds. *Annu. Rev. Astron. Astrophys.* **2006**, *44*, 367−414.